

# Hyperfine structure of the $2^3P$ state in ${}^9\text{Be}$ and the nuclear quadrupole moment

Mariusz Puchalski and Jacek Komasa

Faculty of Chemistry, Adam Mickiewicz University, Uniwersytetu Poznańskiego 8, 61-614 Poznań, Poland

Krzysztof Pachucki

Faculty of Physics, University of Warsaw, Pasteura 5, 02-093 Warsaw, Poland

(Dated: December 23, 2024)

We have performed accurate calculations of the hyperfine structure of the  $2^3P$  state in the  ${}^9\text{Be}$  atom with the help of highly optimized, explicitly correlated functions, accounting for the leading finite nuclear mass, radiative, nuclear structure and relativistic effects. By comparison with measurements, we have determined the  ${}^9\text{Be}$  nuclear quadrupole moment to be  $Q_N = 0.05350(14)$  barns, which is not only the most accurate result, but also disagrees with previous determinations.

The electric quadrupole moment  $Q_N$  of nuclei is a measure of the deformation of the nuclear charge distribution with respect to the spherical symmetry. This deformation comes from a strong dependence of nuclear forces on the orientation of the nucleon spin and is present in atomic nuclei with a spin equal to or greater than one, as it is for  ${}^9\text{Be}$  with  $I = 3/2$ . In principle,  $Q_N$  could be determined from the nuclear structure theory, but such calculations with controlled accuracy have not yet been feasible. Only very recently and only for such a simple nucleus as the deuteron, theoretical predictions based on the chiral effective field theory have reached the uncertainty of 1% [1], and this result agreed with the more precise value from the rotational spectroscopy of the HD molecule [2].

Originally,  $Q_N$  for many nuclei was determined by the electron scattering of the nuclei, for example for  ${}^7\text{Li}$  [3]. However, for  ${}^9\text{Be}$  the available experimental data are not only limited in accuracy but also differ noticeably from each other, indicating that the scattering results are not always conclusive [4, 5]. Nowadays, reliable  $Q_N$  values can be derived from a combination of theoretical and atomic or molecular spectroscopic data. This has been realized for LiH, LiF, and LiCl molecules [6], leading to a  $Q_N({}^7\text{Li})$  consistent with the nuclear scattering value [3]. Although appropriate theoretical calculations were performed for  $\text{BeH}^+$  [7, 8] as well as for the  ${}^{7,9}\text{Be}^-$  anion [9] years ago, there have been no corresponding measurements reported so far. Therefore, the method of choice for finding  $Q_N({}^9\text{Be})$  is atomic spectroscopy.

In the accurate determination of  $Q_N$  from atomic spectroscopy, it is important to understand the electron-nucleus interaction at the fundamental level. Recent advances in measurements of electronic [10] and muonic atoms [11], together with progress in the theoretical description of atomic spectra [12], indicate the importance of the nuclear structure effects. Therefore, accurate knowledge of the nuclear quadrupole moment will give access to details of the electron-nucleus interactions which, so far, have not been visible, like for example the nuclear quadrupole polarizability [13].

The ground state  $2^1S_0$  of Be is fully symmetric; thus, the nuclear quadrupole moment does not lead here to any observable effect. In contrast, in the lowest excited  $2^3P$  level, which is metastable, the hyperfine interactions cause level

splitting, and this splitting can be accurately measured [14]. So, it is atomic structure theory that must interpret the hyperfine structure in terms of the magnetic dipole and the electric quadrupole moments of the nucleus. Still, the same hyperfine interactions that lead to the hyperfine splitting also cause the hyperfine mixing of different  $2^3P_J$  levels. This mixing had been accounted for in Ref. 14 but in a very simplified way. Although the accuracy of these approximations has been questioned [7], consecutive atomic structure calculations, using modern and sophisticated approaches, have relied on these original inaccurate calculations of the hyperfine mixing. An exception is the work by Beloy *et al.* [15], in which this mixing was calculated in the second order of perturbation theory using the relativistic CI+MBPT approach, but its numerical accuracy turned out to be insufficient to obtain  $Q_N$  with a competitive accuracy.

In this work, we employ well-optimized explicitly correlated Gaussian wave functions to have good control over the numerical accuracy. With these wave functions we perform calculations of the  ${}^9\text{Be}$  hyperfine structure, with a complete treatment of the hyperfine mixing of different  $2^3P_J$  levels. Moreover, we fully account for the leading radiative (QED), finite nuclear mass, and nuclear structure effects, while dealing with relativistic and higher order corrections approximately. Our result for the electric quadrupole moment  $Q_N({}^9\text{Be})$  show that all of its previous determinations were not as accurate as claimed, due to a very approximate treatment of the hyperfine mixing and neglect of the radiative (QED) corrections.

*Fine and hyperfine structure Hamiltonian.*—The most accurate approach for light atomic systems solves at first the nonrelativistic Hamiltonian

$$H = \frac{\vec{p}_N^2}{2m_N} + \sum_a \frac{\vec{p}_a^2}{2} - \sum_a \frac{Z}{r_a} + \sum_{a < b} \frac{1}{r_{ab}}, \quad (1)$$

and next includes relativistic effects as a perturbation. Relevant relativistic effects are split into the fine structure Hamiltonian

$$H_{\text{fs}} = Q_1 + Q_2 \quad (2)$$

$$Q_1 = \sum_a \frac{Z\alpha}{4} \vec{\sigma}_a \cdot \left[ \frac{(g-1)}{m^2} \frac{\vec{r}_a}{r_a^3} \times \vec{p}_a - \frac{g}{m m_N} \frac{\vec{r}_a}{r_a^3} \times \vec{p}_N \right]$$

$$+ \sum_{a \neq b} \frac{\alpha}{4m^2} \vec{\sigma}_a \cdot \left[ g \frac{\vec{r}_{ab}}{r_{ab}^3} \times \vec{p}_b - (g-1) \frac{\vec{r}_{ab}}{r_{ab}^3} \times \vec{p}_a \right] \quad (3)$$

$$Q_2 = - \sum_{a < b} \frac{3\alpha g^2}{16m^2} \sigma_a^i \sigma_b^j \left( \frac{r_{ab}^i r_{ab}^j}{r_{ab}^5} - \frac{\delta^{ij}}{3r_{ab}^3} \right) \quad (4)$$

and the hyperfine structure Hamiltonian

$$H_{\text{hfs}} = \vec{I} \cdot \vec{Q} + \frac{3I^i I^j}{I(2I-1)} \frac{Q^{ij}}{6} \quad (5)$$

$$\vec{Q} = \vec{Q}_1 + \vec{Q}_2 + \vec{Q}_3 \quad (6)$$

$$\vec{Q}_1 = \sum_a \frac{1}{3} \frac{Z\alpha g g_N}{m m_N} \vec{\sigma}_a \pi \delta^3(r_a) \quad (7)$$

$$\vec{Q}_2 = \sum_a \frac{Z\alpha g_N}{2m m_N} \frac{\vec{r}_a}{r_a^3} \times \vec{p}_a - \frac{Z\alpha(g_N-1)}{2m_N^2} \frac{\vec{r}_a}{r_a^3} \times \vec{p}_N \quad (8)$$

$$Q_3^j = \sum_a \frac{Z\alpha g g_N}{8m m_N} \sigma_a^i \left( 3 \frac{r_a^i r_a^j}{r_a^5} - \frac{\delta^{ij}}{r_a^3} \right) \quad (9)$$

$$Q^{ij} = - \sum_a \alpha Q_N \left( 3 \frac{r_a^i r_a^j}{r_a^5} - \frac{\delta^{ij}}{r_a^3} \right), \quad (10)$$

where  $\vec{p}_N = -\sum_a \vec{p}_a$  is the nuclear momentum,  $\vec{I}$  is the nuclear spin,  $g$  is the free-electron g-factor,  $Q_N$  is the electric quadrupole moment of the nucleus, and  $g_N$  is the nuclear g-factor

$$g_N = \frac{m_N}{Z m_p} \frac{\mu}{\mu_N} \frac{1}{I}. \quad (11)$$

Leading QED effects are included in the free electron g-factor, while higher order corrections are accounted for as described later on.

Because the hyperfine splittings are only about 100 times smaller than the fine splitting, one cannot assume that hyperfine levels have a definite angular momentum  $\vec{J} = \vec{L} + \vec{S}$ , but only definite  $\vec{L}$  and  $\vec{S}$ . It is convenient therefore to extend the original formulation of the hyperfine splitting by Hibbert in [16] and represent the fine and the hyperfine structure of the  $2^3P$  state in terms of an effective Hamiltonian, instead of expectation values only

$$\begin{aligned} H_{\text{eff}} = & c_1 \vec{L} \cdot \vec{S} + c_2 (L^i L^j)^{(2)} (S^i S^j)^{(2)} \\ & + a_1 \vec{I} \cdot \vec{S} + a_2 \vec{I} \cdot \vec{L} + a_3 (L^i L^j)^{(2)} S^i I^j \\ & + \frac{b}{6} \frac{3(I^i I^j)^{(2)}}{I(2I-1)} \frac{3(L^i L^j)^{(2)}}{L(2L-1)}, \end{aligned} \quad (12)$$

where the coefficients  $a_1, a_2, a_3, b, c_1, c_2$  are independent of  $J$ , but are specific to the particular state. These coefficients can be obtained, for example, from the matrix elements of  $H_{\text{fs}}$  and  $H_{\text{hfs}}$  in the decoupled  $|M_L, M_S\rangle$  or  $|J, M_J\rangle$  basis. Once these coefficients are known, the above Hamiltonian can be diagonalized yielding the hyperfine levels. Alternatively, the hyperfine structure can be represented in terms of  $J$ -dependent  $A_J$  and  $B_J$  coefficients

$$H_{\text{hfs, eff}} = A_J \vec{I} \cdot \vec{J} + \frac{B_J}{6} \frac{3(I^i I^j)^{(2)}}{I(2I-1)} \frac{3(J^i J^j)^{(2)}}{J(2J-1)}, \quad (13)$$

which are conventionally used to represent the measured values, while the fine structure is given in terms of differences in the centroid energies.

If the atomic levels had a definite value  $J$ , the fine structure would be given by the expectation value of  $H_{\text{eff}}$ , namely

$$E_{\text{fs}}(J) = \begin{cases} c_1 + c_2/6 & \text{for } J = 2 \\ -c_1 - 5c_2/6 & \text{for } J = 1 \\ -2c_1 + 5c_2/3 & \text{for } J = 0 \end{cases}, \quad (14)$$

and the hyperfine structure by

$$\begin{aligned} A_J &= \begin{cases} a_1/2 + a_2/2 + a_3/6 & \text{for } J = 2 \\ a_1/2 + a_2/2 - 5a_3/6 & \text{for } J = 1 \end{cases}, \\ B_J &= \begin{cases} b & \text{for } J = 2 \\ -b/2 & \text{for } J = 1 \end{cases}. \end{aligned} \quad (15)$$

Because, in general, one cannot assume that the levels have a definite value of  $J$ , the effective hfs Hamiltonian in Eq. (12) has to be diagonalized numerically. Nonetheless, the hyperfine structure can still be represented in terms of  $A_J$  and  $B_J$  coefficients, and we use them for comparison of theoretical predictions with experimental results and for the determination of the nuclear quadrupole moment  $Q_N$ .

*Relativistic, radiative, and finite nuclear size corrections.*—

The hyperfine Hamiltonian in Eq. (5) represents the leading hyperfine interactions, but there are also many small corrections which are often overlooked in literature. These corrections contain terms with higher powers of the fine structure constant  $\alpha$ . Because most of them are proportional to the Fermi contact interaction, we account for them in terms of the following factor

$$\tilde{a}_1 = a_1(1 + \epsilon). \quad (16)$$

Below, we briefly describe contributions included in the  $\epsilon$  term.

The  $O(\alpha)$  correction is analogous to that in hydrogenic systems [17] and consists of two parts. The first part is due to the nuclear recoil

$$H_{\text{rec}}^{(5)} = \left[ -\frac{3Z\alpha}{\pi} \frac{m}{m_N} \ln\left(\frac{m_N}{m}\right) \right] \vec{I} \cdot \sum_a \frac{2}{3} \frac{Z\alpha g_N}{m m_N} \vec{\sigma}_a \pi \delta^3(r_a) \quad (17)$$

and numerically is very small, almost negligible. The recoil contribution to  $\epsilon$  amounts to  $\epsilon_{\text{rec}} = -0.000011$ . The second part of the  $O(\alpha)$  correction is due to the finite nuclear size and the nuclear polarizability, and is given by [17, 18]

$$H_{\text{fs}}^{(5)} = [-2Z\alpha m r_Z] \vec{I} \cdot \sum_a \frac{2}{3} \frac{Z\alpha g_N}{m m_N} \vec{\sigma}_a \pi \delta^3(r_a), \quad (18)$$

where  $r_Z$  is a kind of effective nuclear radius called the Zemach radius. Disregarding the inelastic effects, this radius can be written down in terms of the electric charge  $\rho_E$  and magnetic-moment  $\rho_M$  densities as

$$r_Z = \int d^3r d^3r' \rho_E(r) \rho_M(r') |\vec{r} - \vec{r}'|. \quad (19)$$

Nevertheless, the inelastic, i.e. polarizability, corrections can be significant, but because they are very difficult to calculate, they are usually neglected. In this work we account for possible inelastic effects by employing  $r_Z$  from a comparison of very accurate calculations of hfs in  ${}^9\text{Be}^+$  with the experimental value, namely  $r_Z = 4.07(5)$  fm [18]. Because this correction is also proportional to the contact Fermi interaction, we represent it in terms of  $\epsilon_{\text{fs}} = -0.000\,615$ .

Next, there are radiative and relativistic corrections of the relative order  $O(\alpha^2)$ . The radiative correction, beyond that included by the free electron g-factor, is [17]

$$H_{\text{rad}}^{(6)} = Z \alpha^2 \left( \ln 2 - \frac{5}{2} \right) \vec{I} \cdot \sum_a \frac{2}{3} \frac{Z \alpha g_N}{m m_N} \vec{\sigma}_a \pi \delta^3(r_a) \quad (20)$$

and the corresponding  $\epsilon$  factor is  $\epsilon_{\text{rad}} = -0.000\,384$ . The  $O(\alpha^2)$  relativistic and higher order corrections are much more complicated. They have been calculated for the ground state of  ${}^9\text{Be}^+$  [18]. Here we take this result and assume that it is proportional to the Fermi contact interaction, and obtain  $\epsilon_{\text{rel}} = 0.001\,664$ . This is the only approximation we assume in this work, and as a consequence we neglect the mixing of the  $2^3P_1$  state with the nearby lying  $2^1P_1$ . Exactly for this reason we will use only the hyperfine splitting of the  $2^3P_2$  state, which does not mix with  $2^1P_1$  for the determination of  $Q_N$ . The resulting total correction is

$$\epsilon = \epsilon_{\text{rec}} + \epsilon_{\text{fs}} + \epsilon_{\text{rad}} + \epsilon_{\text{rel}} = 0.654 \cdot 10^{-3}. \quad (21)$$

Some previous works present these multiplicative correction for all individual hyperfine contributions, but in our opinion this cannot be fully correct because higher order relativistic corrections may include additional terms, beyond that in  $H_{\text{eff}}$  in Eq. (12). These corrections are expected to be much smaller than the experimental uncertainty for the  $B_J$  coefficient, and therefore are neglected.

*ECG wave function and expectation values.*—Let us now move to the calculations of the  $a_i$ ,  $b$ , and  $c_i$  coefficients. To obtain sufficiently high accuracy for these parameters, we express the four-electron atomic wave function as a linear combination of properly symmetrized explicitly correlated Gaussian (ECG) functions,

$$\Psi(\{\vec{r}_a\}) = \sum_{n=1}^K t_n \mathcal{A}[\phi_n(\{\vec{r}_a\}) \chi_{\{a\}}], \quad (22)$$

where  $t_n$  are linear coefficients,  $\mathcal{A}$  is the antisymmetrization operator over electronic indices, and  $\{a\}$  and  $\{\vec{r}_a\}$  denote the sequence of electron indices and coordinates, respectively. The electronic  $P$  symmetry of the states was enforced using the following spatial functions

$$\phi^i(\{\vec{r}_a\}) = r_a^i \exp \left[ - \sum_b w_b r_b^2 - \sum_{c < d} u_{cd} r_{cd}^2 \right] \quad (23)$$

with  $w_b$  and  $u_{cd}$  being nonlinear variational parameters, while the spin functions corresponding to different spin  $S = 1$  projections were, for  $\{a\} = (1, 2, 3, 4)$ :

$$\chi_{\{a\}}^{1-1} = \frac{1}{\sqrt{2}} (\alpha_1 \beta_2 - \beta_1 \alpha_2) \beta_3 \beta_4, \quad (24)$$

$$\chi_{\{a\}}^{10} = \frac{1}{2} (\alpha_1 \beta_2 - \beta_1 \alpha_2) (\alpha_3 \beta_4 - \beta_4 \alpha_3), \quad (25)$$

$$\chi_{\{a\}}^{11} = \frac{1}{\sqrt{2}} (\alpha_1 \beta_2 - \beta_1 \alpha_2) \alpha_3 \alpha_4. \quad (26)$$

To control the uncertainty of our results we performed the calculations with several basis sets successively increasing their size. The nonlinear parameters were optimized variationally with respect to the nonrelativistic energy  $E$  until the energy reached stability in a desired number of digits. From the analysis of convergence we obtained the extrapolated nonrelativistic energies and mean values used in Table I. The largest wave functions optimized variationally were composed of 6144 terms, leading to the nonrelativistic energy in agreement with the result obtained by Kedzierski et al. [19].

The optimized nonrelativistic wave functions were subsequently employed to evaluate the fine and hyperfine parameters from the expectation values of the corresponding quantum-mechanical operators (2)-(10). For this purpose we chose  $J = 2$ ,  $L = 1$ , and for an arbitrary  $M$

$$c_1 = \langle J, M | Q_1 | J, M \rangle, \quad (27)$$

$$c_2 = 6 \langle J, M | Q_2 | J, M \rangle, \quad (28)$$

$$a_1 = \langle J, M | \vec{Q}_1 \cdot \vec{J} | J, M \rangle / 3, \quad (29)$$

$$a_2 = \langle J, M | \vec{Q}_2 \cdot \vec{J} | J, M \rangle / 3, \quad (30)$$

$$a_3 = \langle J, M | \vec{Q}_3 \cdot \vec{J} | J, M \rangle, \quad (31)$$

$$b = \langle L, M | Q^{ij} L^i L^j | L, M \rangle / 5. \quad (32)$$

The numerical values of these parameters and their convergence with increasing size of the ECG basis are shown in Table I. Their relative accuracy can be estimated collectively as better than  $6 \cdot 10^{-6}$ .

*Fine and hyperfine structure.*—The hyperfine transition frequencies  $\nu_J(F; F+1)$  can be expressed in terms of the  $A_J$  and  $B_J$  parameters and vice versa. For this, one writes

$$\langle H_{\text{hfs,eff}} \rangle_F = A_J A_{IJF} + B_J B_{IJF} + C_J C_{IJF} \quad (33)$$

where

$$A_{IJF} = \frac{1}{2} K \quad (34)$$

$$B_{IJF} = \frac{3/4 K(K+1) - I(I+1)J(J+1)}{2I(2I-1)J(2J-1)} \quad (35)$$

with  $K = F(F+1) - I(I+1) - J(J+1)$  and the total angular momentum  $\vec{F} = \vec{S} + \vec{L} + \vec{I}$ . The octupole term  $C_{IJF}$  is given e.g. by Schwartz [22] and Jaccarino [23].

For  $J = 1$  we arrive at

$$A_1 = -\frac{1}{6} \nu_1 \left( \frac{1}{2}; \frac{3}{2} \right) - \frac{3}{10} \nu_1 \left( \frac{3}{2}; \frac{5}{2} \right) \quad (36)$$

$$B_1 = \frac{1}{3} \nu_1 \left( \frac{1}{2}; \frac{3}{2} \right) - \frac{1}{5} \nu_1 \left( \frac{3}{2}; \frac{5}{2} \right), \quad (37)$$

and for  $J = 2$

$$A_2 = -\frac{3}{50} \nu_2 \left( \frac{1}{2}; \frac{3}{2} \right) - \frac{7}{50} \nu_2 \left( \frac{3}{2}; \frac{5}{2} \right) - \frac{4}{25} \nu_2 \left( \frac{5}{2}; \frac{7}{2} \right) \quad (38)$$

TABLE I. Convergence of the nonrelativistic energy and theoretical fine and hyperfine structure parameters for the  $2^3P$  state of  ${}^9\text{Be}$  (in MHz). Mass  $m_N = 9.012\,183\,07(8)$  u [20] and magnetic moment  $\mu/\mu_N = -1.177\,432(3)$  [21] were used for the  ${}^9\text{Be}$  nucleus.

$K$	$E/\text{a.u.}$	$c_1$	$c_2$	$a_1$	$a_2$	$a_3$	$b/Q_N$ (MHz/barn)
1536	-14.566 340 608 5	32 986.385	5 399.032	-231.116 70	-22.698 781	14.788 494	27.150 476
2048	-14.566 341 144 7	32 987.849	5 399.186	-231.126 66	-22.698 923	14.788 389	27.149 896
3072	-14.566 341 380 0	32 989.401	5 399.240	-231.130 99	-22.698 986	14.788 467	27.149 112
4096	-14.566 341 441 5	32 989.854	5 399.190	-231.129 61	-22.699 124	14.788 579	27.148 954
6144	-14.566 341 466 0	32 990.027	5 399.172	-231.128 99	-22.699 186	14.788 630	27.148 898
$\infty$	-14.566 341 474(8)	32 990.2(2)	5 399.15(2)	-231.128 4(6)	-22.699 24(5)	14.788 68(5)	27.148 87(3)

$$B_2 = \frac{2}{5} \nu_2 \left( \frac{1}{2}; \frac{3}{2} \right) + \frac{2}{5} \nu_2 \left( \frac{3}{2}; \frac{5}{2} \right) - \frac{16}{35} \nu_2 \left( \frac{5}{2}; \frac{7}{2} \right) \quad (39)$$

$$C_2 = -\frac{1}{50} \nu_2 \left( \frac{1}{2}; \frac{3}{2} \right) + \frac{1}{50} \nu_2 \left( \frac{3}{2}; \frac{5}{2} \right) - \frac{1}{175} \nu_2 \left( \frac{5}{2}; \frac{7}{2} \right). \quad (40)$$

The above listed parameters (36)-(40) were evaluated us-

TABLE II.  $A_J$ ,  $B_J$ , and  $C_J$  parameters determined using Eqs. (36)-(40) from experimental [14] and theoretical hfs frequencies  $\nu_J$  (in MHz). The experimental values for  $A_2$  and  $B_2$  parameters inferred in this work are more accurate than those presented in the original work [14] because we included the  $C_2$  parameter in their determinations.

	Experimental	Theoretical	Difference
$A_1$	-140.1564(8)	-140.1091	-0.0473(8)
$B_1$	-3.2363(7)	-3.2337	-0.0026(7)
$A_2$	-124.6165(5)	-124.6073	-0.0092(5)
$B_2$	0.7800(21)	0.7800	0.0
$C_2$	-0.00030(9)	-0.00032	0.00002(9)

ing both experimental and theoretical transition frequencies  $\nu_J(F; F+1)$ , and their numerical values are presented in Table II. The experimental values of  $\nu_J$  (in MHz) were taken from Ref. 14, while theoretical ones were found by diagonalization of the effective Hamiltonian of Eq. (12). Most importantly, the parameter  $b$  was fixed by matching theoretical and experimental  $B_2$ , which holds for

$$b = 1.4525(40) \text{ MHz}, \quad (41)$$

where the uncertainty originates from that of the experimental one in  $B_2$ .

The differences between experimental and theoretical values, shown in Tab. II, are not discrepancies but result from neglected higher order relativistic and QED effects, which are beyond those proportional to the Fermi contact interaction. For the  $A_2$  coefficient these effects are of relative order  $0.07 \cdot 10^{-3}$ , while for  $A_1$  they are  $0.33 \cdot 10^{-3}$ . They are larger for  $A_1$  due to hyperfine mixing of  $2^3P_1$  with the nearby  $2^1P_1$  state, which we have not taken into account in our calculation. Moreover, the relative difference for the  $B_1$  coefficient is  $\delta B_1/B_1 = 0.80 \cdot 10^{-3}$ , which most probably is also due to this mixing. For this reason, we have chosen  $B_2$  and not  $B_1$  for the determination of the  $b$  coefficient.

The centroids of the calculated hyperfine energy levels are shown in Tab. III in the column ‘fs levels’ for all  $J$  values of the  $2^3P$  state. This table contains also experimental [14] and calculated fine-structure transition frequencies as well as their difference. This difference originates again from the higher

TABLE III. Theoretical fine structure (fs) energy levels of the  $2^3P$  state of  ${}^9\text{Be}$ , and the comparison of experimental [14] and theoretical fs transition frequencies (in GHz).

$J$	fs levels	$\nu^{\text{exp}}(J; J+1)$	$\nu^{\text{the}}(J; J+1)$	Diff.
2	33.890			
1	-37.489	71.86(24)	71.379	0.48(24)
0	-56.987	19.41(19)	19.498	-0.09(19)

order relativistic and QED effects. Due to a large experimental uncertainty we cannot conclude much about the magnitude of these effects.

*Determination of  $Q_N({}^9\text{Be})$ .*—Having calculated the value of  $b/Q_N = 27.148\,87(3)$  MHz/barn, see Tab. I, and fixed  $b$  by matching theoretical and experimental values of  $B_2$ , we obtain the electric nuclear quadrupole moment  $Q_N$  of  ${}^9\text{Be}$

$$Q_N = 0.053\,50(14) \text{ barn}. \quad (42)$$

The uncertainty in  $Q_N$  comes from the experimental error in the  $\nu_2$  hyperfine frequencies. In this context, the uncertainties from the neglected higher order relativistic and QED effects in the  $b$  parameter, as well as the numerical uncertainties, are much smaller and are not shown.

Among the literature results listed in Tab. IV and depicted in Fig. 1, only the  $Q_N$  reported by Beloy *et al.* [15], thanks to its large uncertainty, agrees with our quadrupole moment. The lack of agreement with the other previous studies indicates that it is very difficult to estimate theoretical uncertainties using well-established, atomic structure methods such as MCHF or CI+MBPT.

*Conclusions.*—We have determined the electric quadrupole moment  $Q_N({}^9\text{Be})$  with significantly higher accuracy and in disagreement with previous values. The improvement achieved in this work has several independent sources. The first one is the recalculation of the  $A_2$ ,  $B_2$ , and  $C_2$  coefficients from experimental hyperfine splitting. More precisely, including  $C_2$  in the effective Hamiltonian  $H_{\text{hfs,eff}}$  in Eq. (13)

TABLE IV. Comparison of the electric quadrupole moment (in barns) of the  ${}^9\text{Be}$  nucleus obtained using atomic structure calculations.

Source	$Q_N({}^9\text{Be})$
Blachman and Lurio, 1967 [14]	0.049(3)
Ray <i>et al.</i> , 1973 [24]	0.0525(3)
Sinanoglu and Beck, 1973 [25]	0.05494
Beck and Nicolaides, 1984 [26]	0.05545
Sundholm and Olsen, 1991 [27]	0.05288(38)
Jönsson and Fisher, 1993 [28]	0.05256
Nemouchi <i>et al.</i> , 2003 [9]	0.05277
Belyov <i>et al.</i> , 2008 [15]	0.053(3)
This work	0.05350(14)

enabled us to decrease the experimental uncertainties by a factor of 2. The second improvement is due to the inclusion of the hyperfine mixing by exact diagonalization of the effective fine- and hyperfine-structure Hamiltonian of Eq. (12). The third improvement comes from the very accurate calculation of the expectation values of the fine- and hyperfine-structure operators using explicitly correlated functions allowing for the complete electron correlations. The fourth one is due to the exact inclusion of the finite nuclear mass in the fine and hyperfine interaction in Eqs. (2) and (5). Finally, the fifth source of improvement is due to accounting for the relativistic, radiative and nuclear structure corrections by appropriate rescaling of the  $a_1$  parameter.

Regarding our theoretical uncertainties, they come exclusively from neglected higher order relativistic and QED contributions, in particular those due to hyperfine mixing of the  $2^3P_1$  and  $2^3P_1$  states. The calculation of the complete  $\mathcal{O}(\alpha^2)$  correction is possible but technically difficult. It has been performed for  $\text{Be}^+$  in [29] due to the possibility to use the exponentially correlated basis functions there. Nevertheless, if a complete  $\mathcal{O}(\alpha^2)$  correction is known, one can use both  $B_1$  and  $B_2$  parameters to obtain an even more accurate nuclear quadrupole moment of  ${}^9\text{Be}$ .

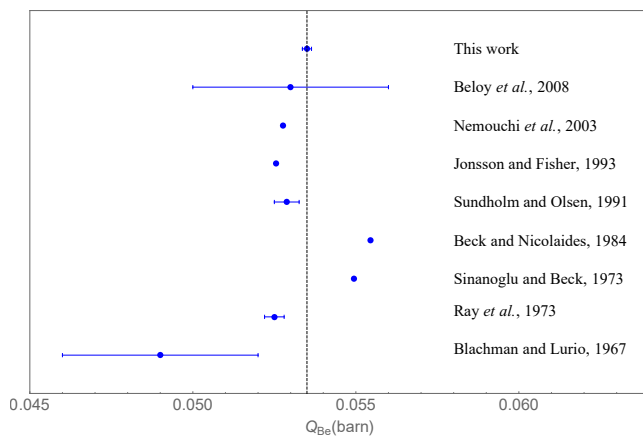


FIG. 1. Comparison of the electric quadrupole moment (in barns) of the  ${}^9\text{Be}$  nucleus obtained using atomic structure calculations.

**Acknowledgments.**—This research was supported by National Science Center (Poland) Grant No. 2014/15/B/ST4/05022 as well as by a computing grant from Poznań Supercomputing and Networking Center and by PL-Grid Infrastructure.

- [1] A. A. Filin, V. Baru, E. Epelbaum, H. Krebs, D. Möller, and P. Reinert, Phys. Rev. Lett. **124**, 082501 (2020).
- [2] M. Puchalski, J. Komasa, and K. Pachucki, Phys. Rev. Lett. **125**, 253001 (2020).
- [3] H.-G. Voelk and D. Fick, Nucl. Phys. A **530**, 475 (1991).
- [4] D. Vinciguerra and T. Stovall, Nucl. Phys. A **132**, 410 (1969).
- [5] M. Bernheim, R. Riskalla, T. Stovall, and D. Vinciguerra, Phys. Lett. B **30**, 412 (1969).
- [6] M. Urban and A. J. Sadlej, Chem. Phys. Lett. **173**, 157 (1990).
- [7] G. H. Diercksen and A. J. Sadlej, Chem. Phys. Lett. **155**, 127 (1989).
- [8] A. C. Borin, F. B. Machado, and F. R. Ornellas, Chem. Phys. Lett. **196**, 417 (1992).
- [9] M. Nemouchi, P. Jönsson, J. Pinard, and M. Godefroid, J. Phys. B **36**, 2189 (2003).
- [10] E. Tiesinga, P. J. Mohr, D. B. Newell, and B. N. Taylor, Rev. Mod. Phys. (2021), in press.
- [11] J. J. Krauth *et al.*, Nature **589**, 527 (2021).
- [12] K. Pachucki, V. Patkóš, and V. A. Yerokhin, Phys. Rev. A **97**, 062511 (2018).
- [13] J. Friar and G. Payne, Phys. Rev. C **72** (2005).
- [14] A. G. Blachman and A. Lurio, Phys. Rev. **153**, 164 (1967).
- [15] K. Belyov, A. Derevianko, and W. R. Johnson, Phys. Rev. A **77**, 012512 (2008).
- [16] A. Hibbert, Rep. Prog. Phys. **38**, 1217 (1975).
- [17] M. I. Eides, H. Grotch, and V. A. Shelyuto, Phys. Rep. **342**, 63 (2001).
- [18] M. Puchalski and K. Pachucki, Phys. Rev. A **79**, 032510 (2009).
- [19] A. Kedzierski, M. Stanke, and L. Adamowicz, Chem. Phys. Lett. **751**, 137476 (2020).
- [20] M. Wang, G. Audi, F. G. Kondev, W. Huang, S. Naimi, and X. Xu, Chin. Phys. C **41**, 030003 (2017).
- [21] N. J. Stone, J. Phys. Chem. Ref. Data **44**, 031215 (2015).
- [22] C. Schwartz, Phys. Rev. **97**, 380 (1955).
- [23] V. Jaccarino, J. G. King, R. A. Satten, and H. H. Stroke, Phys. Rev. **94**, 1798 (1954).
- [24] S. N. Ray, T. Lee, and T. P. Das, Phys. Rev. A **8**, 1748 (1973).
- [25] O. Sinanoglu and D. R. Beck, Chem. Phys. Lett. **20**, 221 (1973).
- [26] D. R. Beck and C. A. Nicolaides, Int. J. Quantum Chem. **26**, 467 (1984).
- [27] D. Sundholm and J. Olsen, Phys. Rev. Lett. **68**, 927 (1992).
- [28] P. Jönsson and C. F. Fischer, Phys. Rev. A **48**, 4113 (1993).
- [29] M. Puchalski and K. Pachucki, Phys. Rev. A **89**, 032510 (2014).